Processing Hemp Shiv Particles for Building Applications: Alkaline Extraction for Concrete and Hot Water Treatment for Binderless Particle Board

Maya-Sétan Diakité, Vincent Lequart, Alexandre Hérisson, Élise Chenot, Sébastien Potel, Nathalie Leblanc, Patrick Martin, Hélène Lenormand

applied sciences

MDPI

Article

Processing Hemp Shiv Particles for Building Applications: Alkaline Extraction for Concrete and Hot Water Treatment for Binderless Particle Board

Maya-Sétan Diakité [1,*], Vincent Lequart [2], Alexandre Hérisson [3], Élise Chenot [4], Sébastien Potel [4], Nathalie Leblanc [5], Patrick Martin [2] and Hélène Lenormand [5,†]

[1] Department of Plant Breeding, Swedish University of Agricultural Sciences, 23053 Alnarp, Sweden
[2] Université d'Artois, UniLaSalle, ULR7519—Transformations & Agro-Ressources, F-62400 Béthune, France; vincent.lequart@univ-artois.fr (V.L.); patrick.martin@univ-artois.fr (P.M.)
[3] UniLaSalle, ULR7519—Unité Transformations & Agro-Ressources, F-60026 Beauvais, France; alexandre.herisson@unilasalle.fr
[4] UniLaSalle, B2R, Geosciences Department, Institut Polytechnique, F-60026 Beauvais, France; elise.chenot@unilasalle.fr (É.C.); sebastien.potel@unilasalle.fr (S.P.)
[5] UniLaSalle, ULR7519—Transformations & Agro-Ressources, F-76130 Mont-Saint-Aignan, France; nathalie.leblanc@unilasalle.fr
* Correspondence: maya.setan.diakite@slu.se
† In memory of our colleague Hélène Lenormand.

Abstract: The building and construction sector is the largest emitter of greenhouse gases, accounting for 37% of global emissions. The production and use of materials such as cement, steel, and aluminum contribute significantly to this carbon footprint. Utilizing valorized agricultural by-products, such as hemp shiv and sunflower pith, in construction can enhance the insulating properties of materials and reduce their environmental impact by capturing CO_2. Additionally, during the formulation process, molecules such as polyphenols and sugars are released, depending on process parameters like pH and temperature. In some cases, these releases can cause issues, such as delaying the hardening of agro-based concrete or serving as binding agents in binderless particle boards. This study focuses on the molecules released during the processing of these materials, with particular attention to the effects of pH and temperature, and the modifications to the plant particles resulting from these conditions. Physical, chemical, and morphological analyses were conducted on the treated hemp shiv particles (HS1 and HS2). No physical or morphological differences were observed between the samples. However, chemical differences, particularly in the lignin and soluble compound content, were noted and were linked to the release of plant substances during the process.

Keywords: hemp shiv; liquid extractions; hemp concrete; binderless particle board; agro-based materials; building; plant cell wall

Citation: Diakité, M.-S.; Lequart, V.; Hérisson, A.; Chenot, É.; Potel, S.; Leblanc, N.; Martin, P.; Lenormand, H. Processing Hemp Shiv Particles for Building Applications: Alkaline Extraction for Concrete and Hot Water Treatment for Binderless Particle Board. *Appl. Sci.* **2024**, *14*, 8815. https://doi.org/10.3390/app14198815

Academic Editor: Syed Minhaj Saleem Kazmi

Received: 19 August 2024
Revised: 11 September 2024
Accepted: 18 September 2024
Published: 30 September 2024

1. Introduction

Lignocellulosic biomass, such as hemp, has been utilized for millennia. Initially, its cultivation focused on fiber production for clothing and ropes used in shipbuilding [1]. Over time, its applications expanded to include animal feed [2], high-value molecules for the pharmaceutical industry [3], second-generation biofuels [4,5], and, more recently, as a raw material for agro-based construction materials [6]. These agro-based products are valued for their insulating properties, minimal carbon footprint, and potential to enhance air quality [7]. Industrial hemp has emerged as a notable crop due to its carbon sequestration capabilities, high biomass yield, and versatile end-use applications [8].

Recent research has explored the incorporation of plant materials into agro-based construction products like particle boards and concrete. During the formulation of these materials [9,10], parameters such as pH, temperature, and pressure influence the release of

various molecules, including polyphenols and sugars [9–12]. These released compounds can either hinder or facilitate the formulation process. For example, studies [10,13–16] have shown that these molecules can affect the hardening of agro-based concrete, either delaying or accelerating the process (Figure 1a).

Bruere (1966) [15] and Taplin et al. (1962) [16] observed that compounds with the HO-C-C=O functional group can retard hardening. Fischer et al. (1974) [17] linked this effect to carbohydrate solubility, while Simatupang et al. (1986) [18] identified hemicellulose solubility as a factor in delaying hardening. Govin et al. (2005) [19] found that, in addition to sugars, polyphenols like vanillic acid and hydroxycinnamic acid can disrupt concrete setting. Diquélou et al. (2015) [20] noted a significant reduction (up to 40%) in Portlandite content in hemp shiv concrete, attributed to the molecules released around the particles. They also observed an interfacial transition zone (ITZ) around the vegetal particles. The ITZ is a gradual region where the composition and microstructure of the binder matrix are influenced by the presence of plant particles. In this zone, extractives compounds from the plant are released, forming a halo around the particles. Red arrows 1 and 2 indicate areas inside and outside of the halo. Nalet (2015) [21] emphasized the importance of diastereoisomers, particularly the R/S positional alternation. More recently, Wang et al. (2019, 2021) [11,12] highlighted how specific sugars (e.g., pectins, glucose) affect concrete hardening, noting that very low sugar concentrations (below 1%) can cause delays. The observed effects are influenced not only by sugar concentration but also by the type of sugar (glucose, fructose, sucrose) [11,12]. Tale Ponga et al. (2023) [22] explores how hemp shiv lixiviates (residual liquid that results from water percolating through a material containing extractives compounds) affect the hydration kinetics and mechanical properties of calcium sulfoaluminate (CSA) cement, a more sustainable alternative to traditional Portland cement. At higher concentrations of up to 5%, the lixiviates were found to slow down the hydration process, especially in General Usage (GU) cement, where the (alite) C_3S hydration was delayed or even inhibited. This resulted in reduced compressive strength. In contrast, CSA cement was less affected by the lixiviates, showing quicker hydration of the aluminate phase and maintaining higher compressive strength. The extractives in the lixiviate had a stronger negative impact on GU (CEM I type) cement's performance, while CSA cement showed better resilience. Thus, the type of cement is another parameter to take into account during the formulation of agro-based concrete.

Despite ongoing research, the exact mechanisms behind these delays are not fully understood, though sugars from hemicellulose and pectins, along with polyphenols, appear to play a significant role.

In the case of binderless particle boards (Figure 1b), the released molecules can act as binding agents between particles. During processing, the combined effects of pressure and temperature lead to the conversion of C_5 and C_6 sugars into furfural derivatives, such as 5-hydroxymethylfurfural (5-HMF) and furfuryl alcohol, which can function as binders [23,24]. Detailed mechanisms of wood particle fusion, known as "Wood Welding", and the interaction of particles without binders, termed "Self-Bonding", have been extensively described [25–28]. A recent comprehensive review [29] has outlined the physical and chemical interactions between cell wall molecules, highlighting that these interactions are primarily related to the degradation of hemicelluloses, cellulose, and lignin into various derivatives. Among these, hemicelluloses play a particularly significant role due to their relative ease of degradation compared to the crystalline structure of cellulose and the complex structure of lignin [30].

Previous studies have established that the composition of cell walls, particularly polysaccharides like hemicelluloses and pectins, as well as polyphenols, significantly impacts the formulation processes (Figure 1). The composition of cell walls can vary widely between hemp shiv samples due to factors such as growing conditions and/or plant varieties. While the types of released molecules are somewhat understood, a more detailed understanding of their interactions during the manufacturing of agro-based materials is still needed. This study aims to mimic the extraction conditions based on pH and

temperature to isolate similar compounds, referred to as "extractives", from two types of hemp shiv: hemp shiv number one called "HS1" and hemp shiv number 2 called "HS2". Previous research [11,13] suggests that HS1 presents challenges for concrete formulation but is promising for binderless particle boards, while HS2 does not exhibit the same issues and seems promising for agro-based concrete. Therefore, these samples were selected for comparison to elucidate the differences in their formulation behavior.

The study focuses on the following two main objectives:

- Physical, morphological and chemical characterization of hemp shiv particles using methods such as the Van Soest method, mass loss measurements, Dynamic Vapor Sorption (DVS), microorganism rate, Scanning Electron Microscopy (SEM), and density assessment.
- Extraction of compounds based on variations in pH and temperature.

The results indicate that while the physical and morphological characteristics do not differentiate between the two types of hemp shiv, their chemical characteristics do provide distinguishing factors.

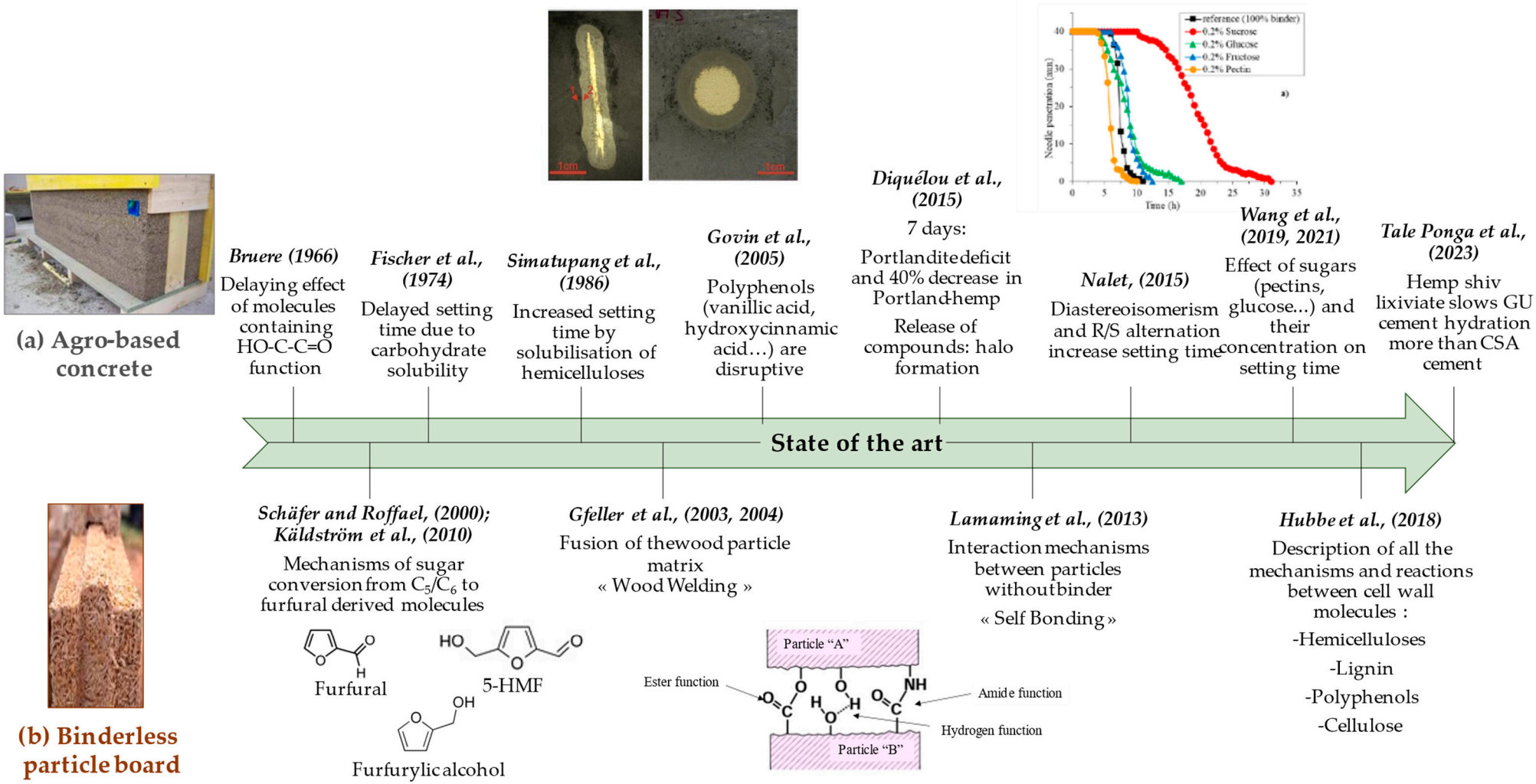

Figure 1. Main historical timeline of the delaying effect of the addition of plant particles in agro-based concrete (**a**) and mechanism of interaction with binderless particle boards (**b**) [11,12,15,17–27,29].

2. Materials and Methods

2.1. Origin and Preparation of Hemp Shiv

This study examines two types of hemp shiv, referred to as HS1 and HS2. HS1 was supplied by Chanvribât, with its variety unidentified, while HS2 came from Ecopertica as the FEDORA17 variety, which was harvested in 2013. Both types of hemp shiv were produced in the Normandy region of France. The production involved defibrating hemp stems at a local processing facility. The resulting hemp shiv particles were sieved to eliminate any residual fibers. Subsequently, a portion of these particles was ground into a fine powder using a mill with a 1 mm sieve for Van Soest analysis, skeletal density measurement, microbial activity and granulometry. The remaining unground hemp shiv particles were stored in an oven at 40 °C.

2.2. Van Soest Method (VS)

The Van Soest method [31] is a comprehensive technique for analyzing cell wall composition and quantifying various components such as cellulose, hemicelluloses, lignin, soluble compounds, and minerals using gravimetric methods. The analysis was conducted using a Fibertec™ 8000 semi-automatic machine (Foss Analytical A/S Company, Hillerød, Denmark) [32].

The process steps and solvents used are described as follows:

(1) Neutral detergent fiber (NDF) (VWR Chemicals, 305,320.5000) was used to remove soluble compounds including pectins, oils, minerals, water, and sugars.
(2) Acid detergent fiber (ADF) (VWR Chemicals, 305,319.5000) was then applied to remove hemicelluloses.
(3) Sulfuric acid (H_2SO_4, 72%) (Carlo Erba Reagents, 502,771) was used to remove cellulose.

After the sulfuric acid treatment, the samples were neutralized with deionized water. Each sample was then dried at 105 °C for 16 h, weighed, and further treated in a furnace at 480 °C for 6 h to eliminate lignin and obtain mineral content. The analysis was performed with six replicates to ensure accuracy [32].

2.3. Microbial Load

The microbial load was assessed in duplicate for the two types of unground hemp shiv using the Aerobic Plate Count (APC) method from NF-V08-059 [33]. This technique measures the level of microorganisms present in the sample. Yeasts and molds were enumerated by counting the colonies incubated at 25 °C on a selective Sabouraud and chloramphenicol medium (SabChl method), which uses chloramphenicol as a selective antibiotic for fungi, yeasts, and molds.

Aerobic microorganisms were determined by counting colonies incubated at 30 °C using the deep plating technique in accordance with Revivable Aerobic Mesophilic Flora Test (RAMF) standards method from NF ISO 4833-1 [34].

2.4. Scanning Electron Microscopy (SEM)

The HS1 and HS2 samples were analyzed with the JSM-IT100 scanning electron microscope (JEOL Technics Ltd., Freising, Germany) and JEOL's InTouchScope™ software (Version 1.090) in BES mode at 15 kV and WD16 mm P.C.60 under a pressure of 40 Pa. The image magnifications chosen were ×500 and ×1000 in longitudinal and transverse sections.

2.5. Granulometry and Densities

Granulometric data for the uncrushed HS1 and HS2, referred to as C3 and C2, were obtained from Vinceslas (2019) [13], as these samples were identical to those used in his study. The samples were arranged and dispersed on a glass surface to prevent particle overlap. Images were captured with a minimum resolution of 600 DPI. Using ImageJ software (Version 1.52). The images were binarized (converted to black and white) and contrasted to measure particle area (mm^2) and width (mm).

Skeletal densities of both ground and unground HS1 and HS2, preconditioned at 40 °C, were measured in triplicate using a helium pycnometer (Pycnomatic Evo, ThermoScientific, Waltham, MA, USA). Apparent density was assessed manually by shaking the uncrushed samples in a glass cylinder ten times and then measuring the sample mass. The volume of water associated with the sample mass was subsequently determined. This process was repeated ten times for each type of hemp shiv [35,36].

2.6. Simulating Process of Agro-Based Materials

2.6.1. Simulation of Agro-Based Concrete: Alkaline Extraction Process

Extractive experiments were conducted in triplicate directly on particle samples. The solid/liquid ratio was 0.01, meaning 3 g of solid material per 300 mL of alkaline solution (NaOH or $Ca(OH)_2$) was adjusted to a pH of 12.5. The extractions were performed at 50 °C for 1 h under agitation at 400 rpm (Table 1).

Table 1. Parameters studied to simulate the preparation conditions of "agro-based concrete".

Conditions of Preparation of the HS1 and HS2/Water Mixture (Ratio = 0.01) for "Agro-Based Concrete" Simulation					
Simulation parameters for extraction	Deionized water 50 °C	NaOH pH 12.5 21 °C	NaOH pH 12.5 50 °C	$Ca(OH)_2$ pH 12.5 21 °C	$Ca(OH)_2$ pH 12.5 50 °C

2.6.2. Simulation of Binderless Particle Board: Hot Water Extraction Process

For the simulation of the binderless particle board process, extractions were carried out under the same conditions as the "agro-based concrete" simulation but with deionized water at either room temperature or 100 °C (Table 2). These extractions were also conducted in triplicate for 1 h, maintaining the same solid/liquid ratio.

Table 2. Parameters studied to simulate the preparation condition of a "binderless particleboard".

Condition of Preparation of the HS1 and HS2/Water Mixture (Ratio = 0.01) for "Binderless Particle Board" Simulation		
Simulation parameters for extraction	Deionized Water 21 °C	Deionized Water 100 °C

During each simulation process (agro-based concrete and binderless particle board), the pH levels were monitored at 0, 30, and 60 min using a pH meter. After 1 h, the samples were filtered and rinsed with milli-Q water. For agro-based concrete simulations, the extractive solution was neutralized with a 1 M HCl solution. All extractive solutions were then freeze-dried to obtain a powder for further analysis.

The treated particles were dried at 105 °C during 16 h, and mass loss measurements were conducted. Subsequently, the particles were analyzed using Dynamic Vapor Sorption (DVS).

2.7. Dynamic Vapor Sorption (DVS)

DVS is a gravimetric technique used to measure changes in sample mass as a function of relative humidity (% rh). This analysis is focused on the adsorption and desorption capacity of the sample. The protocol involves varying the humidity from 0% to 85% at a constant temperature of 23 °C. For adsorption experiments, equilibrium points were determined at 0, 5, 10, 15, 20, 30, 35, 50, 75, and 85% rh. For desorption experiments, equilibrium points were determined at 0, 15, 30, 35, 50, 75, and 85% rh. Each measurement was performed in duplicate using the Sorption Test System from Prolumid [32].

The adsorption and desorption isotherms typically exhibit three distinct regions, corresponding to monolayer adsorption, multilayer adsorption, and liquid water. To model

physical water adsorption, the Brunauer–Emmett–Teller (BET) model [37] was employed, particularly to describe monolayer adsorption at lower relative humidities (0% to 35% rh), which is characteristic of Van der Waals interactions between water molecules and hydrophilic groups (Equation (1)).

$$X_{eq} = \frac{X_m C \varphi}{(1-\varphi)(1+(C-1)\varphi)} \quad (1)$$

The BET model was used to fit the experimental data (equilibrium moisture content, X_{eq}, and relative humidity, φ) to calculate the specific surface area of the sample, a_s (m^2/g) (Equation (2)).

$$a_s = \frac{X_m L a_m}{M_w} \quad (2)$$

where X_m is the monolayer moisture content (kg water/kg dried solid, d.b.) and C is dimensionless. This model assumes that X_m represents the quantity of water molecules required to form a monolayer to cover the entire surface and without diffusion of water through the material.

In the above equation, a_s is the specific surface area of the sample (m^2/g), L is Avogadro's constant (6.023×10^{-23} mol^{-1}), a_m is the cross-sectional area of a water molecule (1.08×10^{-19} m^2) and M_w is the molecular weight of a water molecule (18 $g \cdot mol^{-1}$).

2.8. X-ray Diffraction of Hemp Shiv Particles (XRD)

X-ray diffraction was conducted in duplicate under static conditions, utilizing 256 shots with an angular range from 5° to 40° to determine the percentage of crystalline cellulose. The analysis was performed using a D8 Advance diffractometer (Bruker, Billerica, MA, USA) equipped with a LynxEyes OD detector and a copper anode. Data acquisition was facilitated by Diffrac.eva software (Version 4.2.1).

The crystallinity index of cellulose in HS1 and HS2 was calculated using the Scherrer method, focusing on the second crystallinity peak observed between 18.509° and 27.013°. The average crystallite size was determined using the following equation (Equation (3)) [38]:

$$D(hkl) = \frac{K\lambda}{B_{(hkl)} Cos\theta} \quad (3)$$

In the above equation, $D_{(hkl)}$ is the crystallite size; K is the Scherrer constant (0.9); λ is the X-ray wavelength (0.1542); $B_{(hkl)}$ is the Full Width at Half Maximum (FWHM) of the measured reflection of hkl and 2θ is the Bragg angle.

The objective was to assess the impact of different treatments on cellulose crystallinity.

3. Results and Discussion

3.1. Van Soest Method

The Van Soest results expressed in organic and dry mass are presented in Table 3.

Table 3. Cell wall hemp shiv composition determined by Van Soest method (% w/w). n = 6 with standard variation.

		Cellulose	Hemicelluloses	Lignin	Soluble Compounds	Minerals
HS1	Dry (g ×/100 g dry mass)	49.0 ± 2.8	21.5 ± 1.7	8.1 ± 0.6	18.6 ± 0.8	2.8 ± 0.1
HS2		56.5 ± 2.4	19.7 ± 2.0	12.2 ± 0.8	9.6 ± 0.8	2.0 ± 0.3
HS1	Organic (g ×/100 g organic mass)	50.4 ± 2.8	22.2 ± 1.8	8.3 ± 0.6	19.1 ± 0.8	-
HS2		57.7 ± 2.5	20.1 ± 2.0	12.5 ± 0.8	9.7 ± 0.8	-

The analysis of the chemical composition of hemp shiv samples HS1 and HS2 reveals distinct differences in their cell wall structure. Specifically, HS1 contains 49.0% cellulose, 21.5% hemicelluloses, 8.1% lignin, 18.6% soluble compounds (including pectins, sugars, lipids, and proteins), and less than 3% minerals or ashes. In contrast, HS2 is composed of 56.5% cellulose, 19.7% hemicelluloses, 12.2% lignin, 9.6% soluble compounds, and a similar low mineral content.

The dry mass accounts for both organic and inorganic compounds, while the organic mass considers only the organic components. As a result, the proportion of cell wall compounds increases in the organic mass calculation. HS1 contains 50.4% cellulose, 22.2% hemicelluloses, 8.3% lignin, and 19.1% soluble compounds (including pectins, sugars, lipids, and proteins). In contrast, HS2 is composed of 57.7% cellulose, 20.1% hemicelluloses, 12.5% lignin, and 9.7% soluble compounds.

When comparing these two hemp shiv samples, the cellulose, hemicellulose, and mineral contents are relatively consistent. However, notable differences emerge in the lignin and soluble compound fractions, with HS1 containing about 4% less lignin but 9% more soluble compounds than HS2. These differences in chemical composition could have significant implications for their behavior in agro-based construction materials, particularly in processes such as binderless particle board production or agro-based concrete hardening, where the release of these compounds during processing plays a critical role [11–13].

Literature values for the chemical composition of hemp shiv are generally within the same range as our findings. For instance, previous studies report cellulose content ranging from 44.0% to 51.6%, hemicelluloses from 6.4% to 27.0%, lignin from 8.0% to 28.0%, soluble compounds (including proteins) from 1.0% to 29.4%, and mineral content from 0.6% to 8.8% (Table 4).

Table 4. Cell wall hemp shiv composition by Van Soest method (% w/w) according to literature bibliography.

References	Cellulose	Hemicelluloses	Lignin	Soluble Compounds	Proteins	Minerals
Viel et al., 2018 [39]	49.9	21.4	9.5	17.7		0.6
Thomsen et al., 2005 [40]	48.0	21.0–25.0	17.0–19.0	-	-	-
Garcia-Jaldon, 1995 [41]	48.0	12.0	28.0	7.0	3.0	2.0
Vignon et al., 1995 [42]	44.0	18.0	28.0	5.0	3.0	2.0
Cappelletto et al., 2001 [43]	51.6	21.5	12.9	12.9		6.6
Godin et al., 2010 [44]	47.5	6.4	8.0	29.4		8.8
Gandolfi et al., 2013 [45]	44.0	25.0	23.0	4.0		1.2
Hussain et al., 2018 [46]	44.0	18.0–27.0	22.0–28.0	1.0–6.0	-	1.0–2.0
Arufe et al., 2021 [47]	49.0	21.6	8.1	17.2		4.1
Arufe et al., 2021 [48]	46.1	21.5	8.5	21.1		2.8

The variability observed between different studies, even when using the same analytical technique such as the Van Soest method, underscores the influence of external factors on the chemical composition of hemp shiv.

Several factors may contribute to these variations, including differences in agricultural practices and environmental conditions [39]. For example, variations in pluviometry, climate, and temperature during the growing season can significantly impact the development of the plant's cell wall and, consequently, its chemical composition [39,40]. Such environmental influences could explain why HS1, despite having lower lignin content, shows a higher proportion of soluble compounds [39,40].

These differences in chemical composition between HS1 and HS2 are crucial in understanding their performance in various construction applications. For instance, the lower lignin content and higher soluble compound concentration in HS1 might make it

more susceptible to releasing substances that interfere with concrete setting processes, but these same properties could enhance its self-binding ability in binderless particle boards. Conversely, the higher lignin content in HS2 could contribute to greater structural stability, but with a reduced release of reactive soluble compounds during processing.

Retting, an essential step in the processing of hemp fibers, has been shown to significantly influence the composition of the hemp shiv cell wall. According to Arufe et al. (2021) [48], extended retting, particularly over a 62-day period, results in a notable decrease in the levels of soluble compounds, minerals, and hemicelluloses. This reduction is largely due to the activity of microorganisms, such as fungi and bacteria, that colonize the hemp during retting.

These microorganisms produce specific enzymes, including cellulase, xylanase, xylosidase, mannanase, pectinase, and ligninases, which play a key role in breaking down the lignin–carbohydrate complex (LCC) within the cell walls [30]. By disrupting the covalent bonds within this complex, these enzymes facilitate the degradation of hemicelluloses and pectins, leading to a more disorganized cell wall structure [30]. This enzymatic activity is crucial not only for the separation of fibers but also for altering the chemical profile of the hemp shiv, which can significantly impact its suitability for use in construction materials [48].

To better understand the potential influence of microbial activity on the hemp shiv used in this study, we conducted an analysis to quantify the microbial load in the HS1 and HS2 samples. This analysis is essential for determining how retting and microbial colonization may have affected the chemical composition of these materials, which could, in turn, explain their differing behaviors during the extraction simulations and their performance in applications such as agro-based concrete and binderless particle boards. The results of this microbial analysis will provide insights into the role of these biological processes in shaping the properties of the hemp shiv.

3.2. Microbial Activity

Figure 2a presents the results of the Revivable Aerobic Mesophilic Flora Test (RAMF) conducted at 30 °C. This test serves as an indicator of mesophilic flora, allowing for the enumeration of microorganisms present in the hemp shiv samples. The results are expressed in Colony Forming Units (CFUs), which provide a quantitative measure of the viable microorganisms capable of growing and forming colonies under the specified conditions.

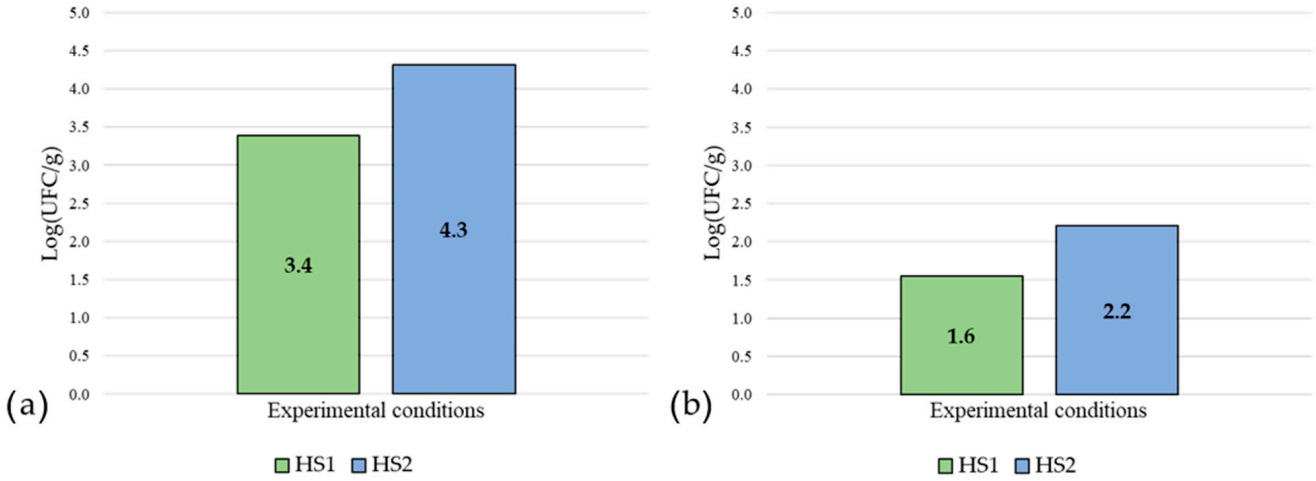

Figure 2. Microbiological tests of HS1 and HS2. FMAR test at 30 °C (**a**) and SABChl at 72 h (**b**).

HS1 exhibits a lower microbial load compared to HS2, with log(CFU/g) values of 3.4 for HS1 against 4.3 for HS2 (Figure 2a). The results of the enumeration on selective Sabouraud and chloramphenicol medium (Figure 2b), which quantifies fungi such as yeasts and molds, reflect a similar trend. Specifically, HS1 shows a log(CFU/g) of 1.6, while HS2

registers a higher value of 2.2 (Figure 2b). The quantitative results indicate that HS1 actually has fewer CFUs than HS2, and by extension, a lower overall microbial load (Figure 2).

The SABChl values are below the threshold value of log(CFU/g) = 2.85 [34], suggesting a relatively low fungal presence. However, when comparing these values with the FMAR results, it appears that some fungi may still be included within the broader mesophilic microorganism count. This suggests that among the mesophilic microorganisms, fungi are likely present but in numbers that remain below the established threshold [34].

These low levels of microorganisms could be attributed to the pre-treatment of the hemp shiv, which involved heating the material at 105 °C for 16 h upon receipt. This treatment was likely intended to stabilize the material, potentially inducing a lifting of dormancy in some microorganisms. As a result, the detected microorganisms might primarily represent those originating from the soil microbiome.

Recent studies have highlighted the existence of bacterial–fungal interactions (BFIs) [49] where microorganisms coexist, which sometimes benefit from or antagonize one another in their environment [50]. These interactions enable both physical and metabolic interdependence [49–51].

The results from the microbiological tests (SabChl and FMAR) point to a potential cohabitation of microorganisms. Consequently, Scanning Electron Microscopy analysis was conducted to visualize bacterial or fungal spores, providing further insight into this possible coexistence.

3.3. Microscopical Analysis by Scanning Electron Microscopy (SEM)

Figures 3 and 4 present transverse and frontal SEM images of HS1 and HS2, respectively. These images facilitate the observation of the shape and size of cell types within a hemp shiv particle, including parenchyma cells, dotted vessels, spiral tracheids, and round microorganisms that appear to be either bacteria or spores aggregated within the parenchyma cells (cluster of microorganisms encircle in red in Figure 3). Some artifacts (encircle in red in the Figure 4), which are unintended features likely caused by the sample preparation process, have also been observed on the surface of the hemp shiv (Figure 4).

The SEM images of HS1 (Figure 3) reveal a higher concentration of microorganisms compared to HS2 (Figure 4). A variety of vessel sizes, ranging from 15 to 60 µm, can be observed. Although the hemp shiv samples were not retted, it is plausible that these microorganisms originated from the soil. Previous studies have highlighted fungi as a significant component of the microflora, particularly in retted hemp, while other research has suggested the coexistence of two microbial communities' bacteria such as *Pseudomonas* and *Escherichia coli*, and fungi like *Cryptococcus* and *Cladosporium* [49]. Furthermore, optical microscopy identified colonies of *Penicillium* and *Aspergillus* types within the samples, which are known to contribute to the enzymatic hydrolysis of pectins through the action of pectinases (including polygalacturonases, pectin lyases, and pectin esterases). The clusters observed in the SEM images may consist of these fungi and bacteria, reinforcing the potential for bacterial–fungal interactions (BFIs) as discussed earlier [49,50].

Additionally, the cell wall images reveal the porosity of the hemp shiv samples. Once dried, the plant material's pores trap air, contributing to the lightness of the material and resulting in low thermal conductivity expressed in Watts per meter Kelvin, making it an effective insulator. These physical characteristics can be further explored through density measurements.

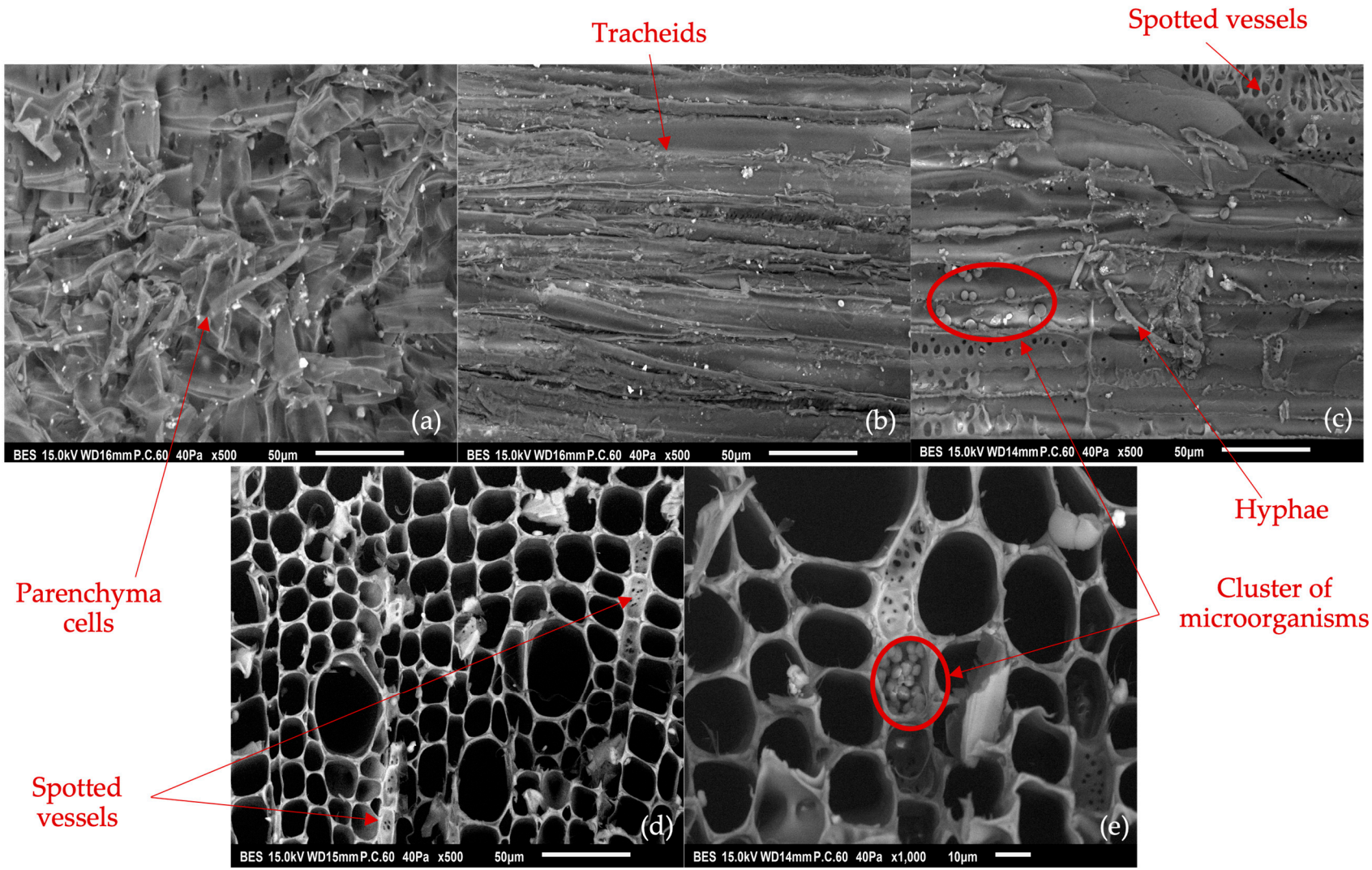

Figure 3. SEM images of HS1 at ×500 and ×1000 magnification in longitudinal (**a**–**c**) and transverse (**d**,**e**) sections. The imaging parameters are presented below each image.

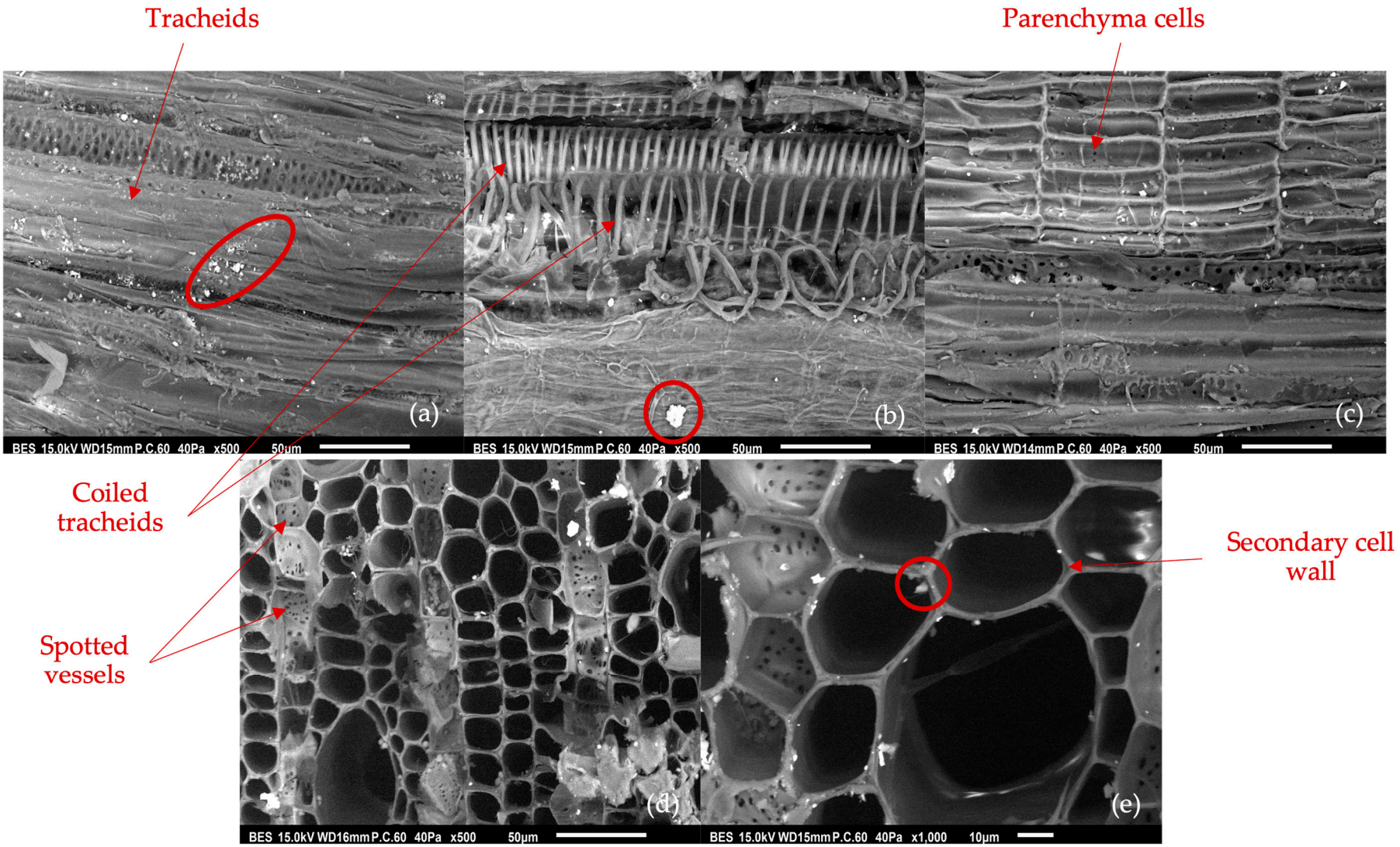

Figure 4. SEM images of HS2 at ×500 and ×1000 magnification in longitudinal (**a**–**c**) and transverse (**d**,**e**) sections. The imaging parameters are presented below each image.

3.4. Physical Characterisation: Granulometry and Densities

The grain size distribution of HS1 and HS2 was analyzed and reported in the thesis of Vinceslas (2019) [13]. HS1 (referred to as C3) and HS2 (referred to as C2) exhibit notable differences in particle dimensions. HS2 has a wider size range compared to HS1, with particle widths ranging from 0.4 to 9 mm for HS2 and from 0.2 to 4 mm for HS1. Additionally, HS2 particles can reach lengths up to 45 mm, whereas HS1 particles vary between 1.5 and 20 mm. Vinceslas (2019) [13] categorizes HS1 as having a "fine" grain size and HS2 as having a "coarse" grain size.

The apparent and skeletal densities of HS1 and HS2 are summarized in Table 5.

Table 5. Apparent and skeletal densities measured for HS1 and HS2.

	Apparent Density	Skeletal Density
HS1	135.1 ± 4.9	1338.4 ± 1.1
HS2	103.0 ± 5.5	1331.0 ± 3.5

The apparent densities of HS1 and HS2 are 135.1 and 103.0 $kg \cdot m^{-3}$, respectively, and their respective skeletal densities are 1338.4 and 1331.0 $kg \cdot m^{-3}$.

These density values are generally consistent with those reported in the scientific literature, although they tend to be slightly lower. For instance, Arufe et al. (2021) [47] and Nguyen et al. (2010) [52] reported apparent densities of 114 kg/m^3 and 113 kg/m^3, respectively, for hemp shiv, which are somewhat lower than the values observed in this study. Similarly, the skeletal densities reported by Delannoy et al., (2018) [53], Amziane and Collet (2018) [35], and Arufe et al. (2021) [47] are 1480 kg/m^3, 1450 kg/m^3, and 1247 kg/m^3, respectively. These values are notably higher than those found in HS1 and HS2.

The discrepancies between the observed densities and those reported in the literature may arise from variations in the processing methods, sample preparation, and environmental conditions during growth and processing. The higher apparent density of HS1 compared to HS2 suggests that HS1 has a denser packing of particles or a smaller proportion of voids between particles.

3.5. Simulating Agro-Based Materials Production

3.5.1. Agro-Based Concrete Simulation—Alkaline Extraction

- pH monitoring during alkaline extraction

The pH values measured at 0, 30, and 60 min for each condition in the "agro-based concrete" simulation are summarized in Table 6. The conditions include milli-Q water at room temperature (RT) and 50 °C, as well as alkaline extractions using NaOH or $Ca(OH)_2$ at a pH of 12.5. These data allow us to evaluate the effects of temperature and alkaline conditions on pH changes.

For the extraction at room temperature (RT), no significant pH differences were observed between HS1 and HS2, nor between the measurements taken at 0 and 60 min. Initially, the pH for both types of hemp shiv was 5.60 for HS1 and 5.66 for HS2, and after 60 min, the pH slightly shifted to 5.65 for HS1 and 5.64 for HS2. However, when the temperature was increased to 50 °C, the pH behavior differed between the two samples. For HS1, the pH decreased from 5.86 to 5.64, indicating a drop of about 0.22 pH units. This suggests that HS1 released acidic compounds, potentially acidic sugars such as galacturonic or glucuronic acids, derived from the breakdown of pectins. In contrast, the pH of HS2 unexpectedly increased from 5.81 to 6.27, a rise of almost 0.5 pH units. This suggests the release of basic and/or neutral compounds, indicating a different chemical response to elevated temperatures compared to HS1.

Table 6. Average pH monitoring at 0, 30 and 60 min of extraction simulating process for "agro-based concrete" simulation in HS1 and HS2.

Time (Minute)	0	30	60	Δ_{0-60}
HS1 RT	5.60	5.66 ± 0.02	5.65 ± 0.02	0.05
HS2 RT	5.66	5.63 ± 0.02	5.64 ± 0.02	0.02
HS1 50 °C	5.86	5.67 ± 0.02	5.64 ± 0.04	0.22
HS2 50 °C	5.81	6.26 ± 0.03	6.27 ± 0.03	0.46
		NaOH		
HS1 NaOH RT	12.50	12.13 ± 0.02	12.08 ± 0.01	0.42
HS2 NaOH RT	12.47	12.38 ± 0.01	12.34 ± 0.01	0.13
HS1 NaOH 50 °C	12.50	11.61 ± 0.07	11.32 ± 0.16	1.18
HS2 NaOH 50 °C	12.47	11.85 ± 0.04	11.67 ± 0.04	0.8
		$Ca(OH)_2$		
HS1 $Ca(OH)_2$ RT	12.50	12.26 ± 0.006	12.23 ± 0.020	0.27
HS2 $Ca(OH)_2$ RT	12.48	12.34 ± 0.006	12.20 ± 0.015	0.28
HS1 $Ca(OH)_2$ 50 °C	12.50	11.52 ± 0.015	11.30 ± 0.025	1.2
HS2 $Ca(OH)_2$ 50 °C	12.48	11.34 ± 0.026	11.13 ± 0.035	1.35

For NaOH solution at room temperature, the pH of HS1 decreases from 12.50 to 12.08, representing a decrease of 0.42 pH units. HS2 shows a smaller decrease from 12.47 to 12.34, a change of 0.13 pH units. When the temperature is raised to 50 °C, HS1's pH drops by 1.18 pH units to 11.32. HS2 experiences a decrease of 0.8 pH units to 11.67.

The combined effect of NaOH and elevated temperature results in a greater pH reduction compared to room temperature conditions, with HS1 showing a decrease of 1.18 pH units and HS2 a decrease of 0.80 pH units. This demonstrates that the increase in both pH and temperature results in a more significant reduction in pH.

For $Ca(OH)_2$ at room temperature, HS1's pH decreases from 12.50 to 12.23, a change of 0.27 pH units. HS2's pH drops from 12.48 to 12.20, a decrease of 0.28 pH units. At 50 °C, HS1's pH falls to 11.30, reflecting a decrease of 1.20 pH units, while HS2's pH decreases to 11.13, a reduction of 1.35 pH units. HS1 seems more sensitive to the NaOH base, while HS2 is more sensitive to $Ca(OH)_2$.

The observed differences in reaction kinetics between HS1 and HS2, depending on the alkaline base and temperature, can be attributed to the distinct chemical compositions of the hemp shiv samples (Tables 3 and 4). At pH 12.50, the main components extracted are hemicelluloses, lignin, polyphenols, and pectins. These compounds interact with Ca^{2+} or Na^{+} ions through ionic bonding, either in their carboxylate forms for saccharides or through non-bonding electron pairs on oxygen atoms [32]. Given that HS2 contains more lignin and polyphenols compared to HS1, while HS1 has a higher sugar content, it is likely that HS1 releases more sugars that interact with Na^{+} under basic conditions, whereas HS2 releases more polyphenols that interact with Ca^{2+}. Competitive interactions between the released compounds and the base, due to differences in chemical composition, may also influence the pH changes observed.

Homogalacturonan chains in pectins can exist in either a methyl-esterified or demethylesterified form. When two chains of galacturonic acid are demethylesterified, they are able to interact with surrounding calcium ions, forming a stable and rigid structure known as the "egg-box" model [54]. This egg-box structure is facilitated by the binding of calcium (Ca^{2+}) to the carboxyl groups of adjacent demethylesterified galacturonic acid residues, creating cross-links between the chains. In the context of lime ($Ca(OH)_2$) extraction, the calcium present in the solution could promote the formation of these egg-box structures, further stabilizing the pectin network. This interaction may impact the overall

structural integrity of the plant material, influencing its behavior in the formulation of agro-based concrete and particle board composites.

- Hemp shiv mass losses

Mass losses were taken before and after extraction and the results are presented in Figure 5.

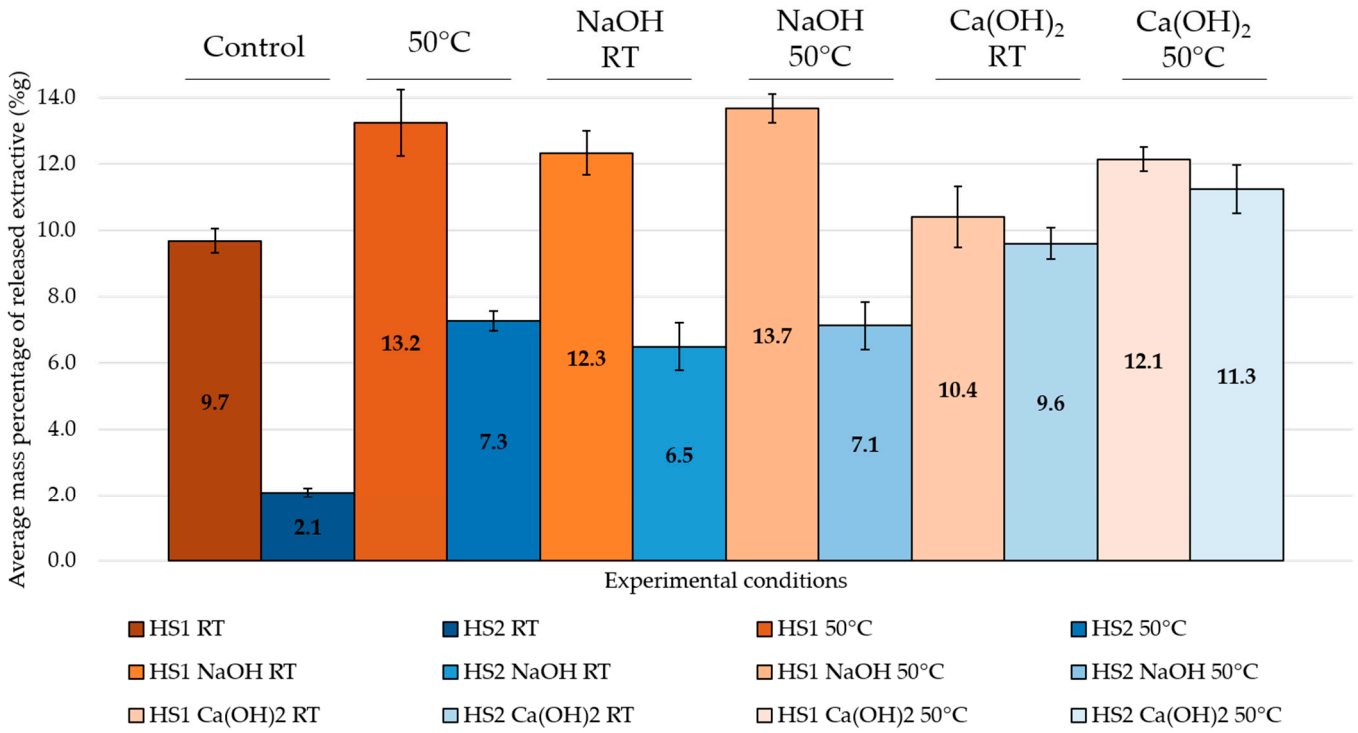

Figure 5. Mass losses of HS1 and HS2 after simulating process extraction of "agro-based concrete" simulation. HS1 is represented in orange shades, while HS2 is represented in shades of blue.

The mass losses at room temperature (RT) were 9.7% for HS1 and 2.1% for HS2. When the temperature was increased to 50 °C, the mass losses for HS1 increased to 13.2% and to 7.3% for HS2. The results for NaOH extraction, both at RT and at 50 °C, were similar, showing mass losses of approximately 13% for HS1 and 7% for HS2. In contrast, $Ca(OH)_2$ extractions resulted in approximately 10% mass loss at RT for both hemp shiv samples, which increased to around 12% with temperature for both HS1 and HS2.

The mass losses observed ranged from 9.7% to 13.7% for HS1 and from 2.1% to 11.3% for HS2, depending on the extraction conditions. These results indicate that temperature has a more significant effect on extraction efficiency compared to the choice of base. Specifically, the mass losses at 50 °C were comparable to those achieved with NaOH, regardless of temperature, suggesting that NaOH is a more effective extraction agent than $Ca(OH)_2$.

The cumulative effect of both pH and temperature does not contribute significantly to increased mass losses or the release of extractive compounds. Nevertheless, HS1 generally releases more extractive compounds compared to HS2 under all conditions, except for the $Ca(OH)_2$ extractions, both with and without temperature.

The variability observed in the results may be influenced by the origin of the hemp shiv, which is not well documented. According to Van Soest's method [31], factors such as biomass variety, cultivation conditions, storage, and age can significantly impact the chemical composition and extractive yields. Therefore, differences in these factors could explain the observed variations in mass losses and extractive compound release between HS1 and HS2.

To further understand the material properties of hemp shiv and the effects of the extraction processes, the specific surface area of the plant material was measured using Dy-

namic Vapor Sorption (DVS). The Brunauer–Emmett–Teller (BET) model was employed to analyze the specific surface area based on the sorption data obtained. The BET model helps in quantifying the surface area by fitting the experimental data to predict the monolayer adsorption capacity, which can provide a comprehensive understanding of the material's surface properties and its interaction with water.

- Specific surface area (a_s)

  The specific surface area values (BET model) are presented in Table 7.

Table 7. Specific surface area (a_s) expressed in m^2/g for "agro-based concrete" simulation.

	Control	50 °C	NaOH RT	NaOH 50 °C	$Ca(OH)_2$ RT	$Ca(OH)_2$ 50 °C
HS1	157.9	171.1	182.5	172.7	151.7	153.3
HS2	153.2	145.0	173.0	146.1	167.0	153.6

For HS1, the specific surface areas measured under different conditions are as follows: 157.9 m^2/g for the control, 171.1 m^2/g for milli-Q water at 50 °C, 182.5 m^2/g for NaOH at room temperature (RT), 172.7 m^2/g for NaOH at 50 °C, 151.7 m^2/g for $Ca(OH)_2$ at RT, and 153.3 m^2/g for $Ca(OH)_2$ at 50 °C. The presence of NaOH tends to increase the specific surface area of HS1, while lime ($Ca(OH)_2$) results in a slight decrease compared to the control condition at room temperature.

Given that the extraction was performed on unground plant particles, it is the external surface of the particles, as well as the open pores accessible to the solvent, that interact with the extraction solvent. Overall, few significant differences were observed between the various conditions for HS1, except that the lime treatments generally resulted in a reduction in specific surface area. Heat (50 °C) also appears to enhance the specific surface area, likely due to the extraction process making water-soluble polar compounds more accessible. Interestingly, when considering the cumulative effects of temperature and base, the specific surface area decreases by approximately 5% for NaOH but increases by about 1% for $Ca(OH)_2$ compared to the base at room temperature.

For HS2, the specific surface area values are 153.2 m^2/g for the control, 145.0 m^2/g for water at 50 °C, 173.0 m^2/g for NaOH at RT, 146.1 m^2/g for NaOH at 50 °C, 167.0 m^2/g for $Ca(OH)_2$ at RT, and 153.6 m^2/g for $Ca(OH)_2$ at 50 °C. A notable trend emerges when comparing the condition with water at 50 °C and the simulations carried out with a base at 50 °C. Interestingly, when considering the cumulative effects of temperature and base, the specific surface area decreases by approximately 15% for NaOH but increases by about 8% for $Ca(OH)_2$ compared to the base at room temperature. HS2 shows similar reaction kinetics under these conditions. This observation suggests that the effect of the base might be negligible when the temperature effect is predominant. However, in the absence of a temperature effect, a tendency for the specific surface area to increase is observed (173.0 m^2/g for NaOH and 167.0 m^2/g for $Ca(OH)_2$). The type of base seems also to be an important factor since we observed those differences between HS1 and HS2.

These results differ significantly from those of HS1 (182.5 m^2/g for NaOH and 151.7 m^2/g for $Ca(OH)_2$), indicating that if the specific surface area of HS2 decreases during the combined base and temperature effects, HS2 may interact less with its environment compared to HS1, leading to a reduced ability to release compounds. This could be a part of the explanation about the difference in the soluble compound rate in Van Soest results between HS1 and HS2 (Table 3).

The specific surface area measurements offer insights into how the hemp shiv interacts with various extraction conditions, shedding light on the material's porosity and surface reactivity. To further elucidate these interactions, X-ray diffraction (XRD) analysis was conducted to examine the crystalline structure of the hemp shiv under different conditions. This analysis will help determine whether changes in surface area correlate with alter-

ations in the crystalline phases of the material, thereby providing a more comprehensive understanding of the effects of temperature and alkaline treatment on hemp shiv.

- X-ray diffraction of hemp shiv particles

X-ray diffraction (XRD) analysis provides valuable insights into the crystallinity of cellulose in hemp shiv, particularly through the calculation of the Scherrer index [55]. This index helps quantify the percentage of crystalline regions within the cellulose structure. In the context of simulating agro-based concrete by liquid extraction, alkaline treatments with $Ca(OH)_2$ and NaOH, applied at either room temperature (RT) or 50 °C, facilitate the hydrolysis of non-crystalline compounds such as lignin, hemicelluloses, and pectins. This hydrolysis enhances the accessibility of cellulose, potentially affecting its crystallinity. The results of the cellulose crystallinity are presented in Figure 6.

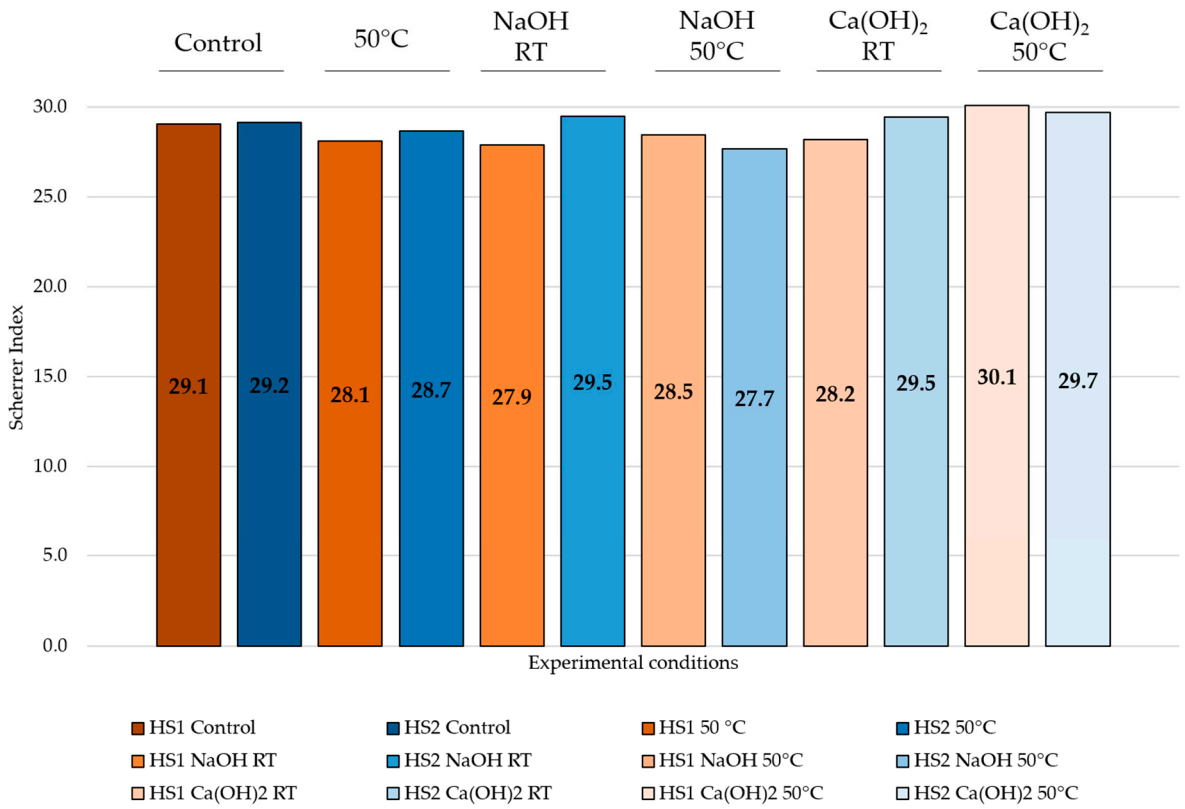

Figure 6. Percentage of crystallinity of HS1 and HS2, measured after applying the conditions of the "agro-based concrete" simulation. HS1 is represented in orange shades, while HS2 is represented in shades of blue.

For HS1, the crystallinities under various treatment conditions are presented in Figure 6. The control sample exhibits a crystallinity of 29.1%, serving as a baseline. When treated with water at 50 °C, the crystallinity of HS1 slightly decreases to 28.1%. Treatment with NaOH at RT results in a crystallinity of 27.9%, which remains nearly unchanged when the temperature is increased to 50 °C (28.5%). Similarly, when $Ca(OH)_2$ is applied at RT, the crystallinity is 28.2%, but this increases to 30.1% when the temperature is raised to 50 °C. The overall variation in crystallinity across all conditions for HS1 ranges from 27.9% to 30.1%, indicating a relatively stable crystallinity except for a noticeable increase in the $Ca(OH)_2$ treatment at 50 °C. This suggests that the combination of base and or elevated temperature does not change the cellulose crystallinity. Similar results are also found in the literature. Momeni et al. (2021) found a crystallinity of 27.1% in untreated hemp shiv powder [55].

HS2 displays different crystallinity trends under similar conditions (Figure 6). The control sample for HS2 shows a crystallinity of 29.2%. When treated with water at 50 °C, the crystallinity slightly decreases to 28.7%. NaOH at RT increases the crystallinity to 29.5%, but when the temperature is raised to 50 °C, a significant drop to 27.7% is observed. $Ca(OH)_2$ treatments, both at RT and 50 °C, maintain higher crystallinity levels at 29.5% and 29.7%, respectively. The variation in crystallinity for HS2 across these conditions ranges from 27.7% to 29.7%, with an increase occurring with NaOH at 50 °C, $Ca(OH)_2$ at RT and $Ca(OH)_2$ at 50 °C.

These differences between HS1 and HS2 (Figure 6) suggest that the type of base and the temperature interact differently with each sample, potentially due to variations in their chemical compositions or structural properties. For HS1, the increase in crystallinity with $Ca(OH)_2$ at 50 °C contrasts with the decrease observed in HS2 when treated with NaOH at the same temperature. This indicates that the origin and specific composition of the hemp shiv may influence how these materials respond to alkaline treatments and temperature changes. However, the observed differences are mainly trends. Ghosn et al. (2020) [56] similarly noted that the intensity of the major XRD peak, which correlates with fiber crystallinity, varies between untreated and treated hemp fibers. Their study found that alkali treatments marginally increased cellulose crystallinity from 70.35% in untreated fibers to 73.20% after alkali treatment [56,57]. Once again, only a trend was observed.

This slight enhancement in crystallinity could help explain the trends observed in our study, particularly the effects of NaOH and $Ca(OH)_2$ without the additional influence of temperature.

3.5.2. Binderless Particle Board Simulation—Hot Water Extraction

- pH monitoring during hot water extraction

The pH values measured at 0, 30, and 60 min for each condition in the "binderless particle board" simulation are summarized in Table 8. The conditions include milli-Q water at room temperature (RT) and 100 °C. This aim is to evaluate the effects of temperature on pH changes.

Table 8. pH monitoring at 0, 30 and 60 min of extraction simulating process for "binderless particle board" simulation in HS1 and HS2.

Time (min)	0	30	60	Δ_{0-60}
HS1 RT	5.60	5.66 ± 0.02	5.65 ± 0.02	0.05
HS2 RT	5.66	5.63 ± 0.02	5.64 ± 0.02	0.02
HS1 100 °C	6.21	5.75 ± 0.05	5.61 ± 0.08	0.60
HS2 100 °C	6.24	6.53 ± 0.12	6.77 ± 0.15	0.53

In the case of extractions conducted at room temperature, the pH for both types of hemp shiv remained stable at approximately 5.6 (Table 8). However, when the extraction temperature was increased to 100 °C, the initial pH of 6.21 for HS1 decreased to 5.61, indicating a drop of 0.60. Conversely, for HS2, the pH increased from 6.24 to 6.77, reflecting a rise of about 0.53. Notably, no significant pH change was observed between HS1 at room temperature and HS1 at 100 °C at 60 min, and both stabilized at a pH of around 5.6. In contrast, a slight increase in pH was observed in HS2 at 100 °C compared to its room temperature control condition after the same period.

The pH decrease in HS1 at 100 °C between 0 and 60 min could be attributed to the release of highly methyl-esterified pectins, which are composed of uronic acids such as galacturonic acid and glucuronic acid. These compounds can be extracted with boiling water, as noted in previous studies [58–60]. Additionally, the drop in pH might also be due to the release of phenolic acids, including chlorogenic acid, vanillic acid, caffeic acid, p-coumaric acid, ferulic acid, and gallic acid, all of which are known to be present in

hemp [61–64]. On the other hand, the slight pH increase observed in all replicates of HS2 at elevated temperatures is a phenomenon that remains unclear. It suggests that HS2 may release fewer uronic or phenolic acids compared to HS1, which would otherwise contribute to a pH decrease. Instead, HS2 might be releasing more neutral compounds, such as water-soluble tannins, flavonoids, or neutral oses like D-glucose, D-xylose, and D-galactose, which could account for the observed pH rise.

- Hemp shiv mass losses

  Hemp shiv mass losses are presented in Figure 7.

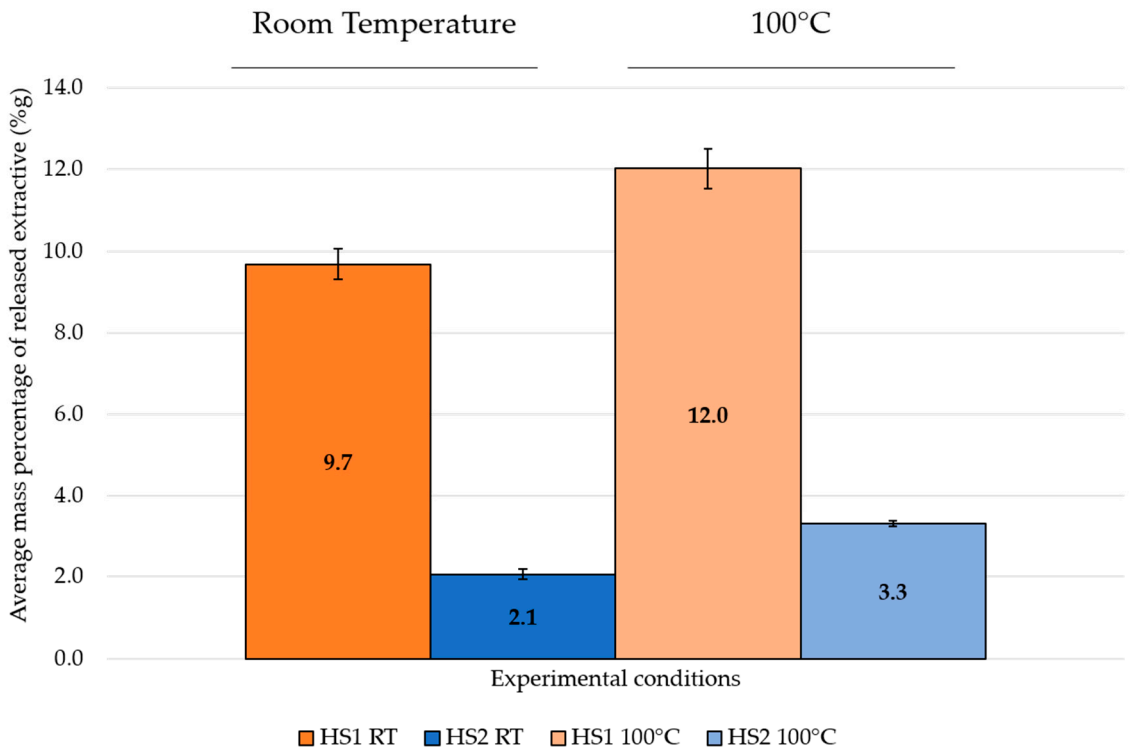

Figure 7. Mass losses of HS1 and HS2 after simulating process extraction of "binderless particle board" simulation. HS1 is represented in orange shades, while HS2 is represented in shades of blue.

The mass losses at room temperature (RT) are 9.7% for HS1 and 2.1% for HS2. When the temperature is increased to 100 °C, the mass losses rise to 12.0% for HS1 and 3.3% for HS2. As consistently observed, HS1 releases more compounds than HS2. These released compounds could be part of the soluble fraction, which is more readily extracted by polar solvents such as water. At 100 °C, these compounds could include methyl-esterified pectins [59,60] and polyphenols such as chlorogenic acid, vanillic acid, or caffeic acid [62].

The increased mass loss suggests that more surface area is exposed as these compounds are released. To better understand the effects of these extractions on the material's physical properties, we can examine the specific surface area of the hemp shiv by utilizing Dynamic Vapor Sorption (DVS) analysis and the Brunauer–Emmett–Teller (BET) model.

- Specific surface area (a_s)

  The specific surface area data are presented in Table 9.

Table 9. Specific surface area (a_s) expressed in m^2/g for "binderless particle board" simulation.

	Control	RT	100 °C
HS1	157.9	164.3	166.3
HS2	153.2	171.7	139.3

HS1 at room temperature (RT) exhibits a specific surface area of 164.3 m^2/g, which slightly increases to 166.3 m^2/g when the temperature is elevated to 100 °C. HS2 demonstrates a decrease in specific surface area from 171.7 m^2/g at RT to 139.3 m^2/g at 100 °C, which represents a decrease of almost 19%. This reduction in surface area for HS2 at higher temperatures suggests a possible structural change or rearrangement of the material, which may reduce the number of accessible pores or reactive sites.

Comparing the specific surface area of HS1 and HS2 under these conditions reveals some interesting trends. HS2 RT shows a slightly higher specific surface area (171.7 m^2/g) than HS1 RT (164.3 m^2/g), indicating that after extraction with water at room temperature, HS2 might initially have a more porous structure. Moreover, when comparing these values to the control samples, the HS1 control has a specific surface area of 157.9 m^2/g and the HS2 control has an area of 153.2 m^2/g. The removal of water-soluble compounds during the heating process leads to an increase in the specific surface area for HS1 and a decrease for HS2. This increase implies that the extraction process may expose more surface area by removing occluding substances, enhancing the material's capacity to interact with other molecules for HS1. On the other hand, the decrease observed in HS2 could be due to the rearrangement of the material, which may hinder the accessibility of open pores.

To gain a deeper understanding of how these structural changes affect the crystallinity of the material, we turn to X-ray diffraction analysis. XRD can provide insights into the degree of crystallinity within the hemp shiv, particularly how alkaline treatments and temperature variations influence the crystalline and amorphous regions of the material.

- X-ray diffraction of hemp shiv particles

The percentages of crystallinity for the hemp shiv particles HS1 and HS2 are illustrated in Figure 8.

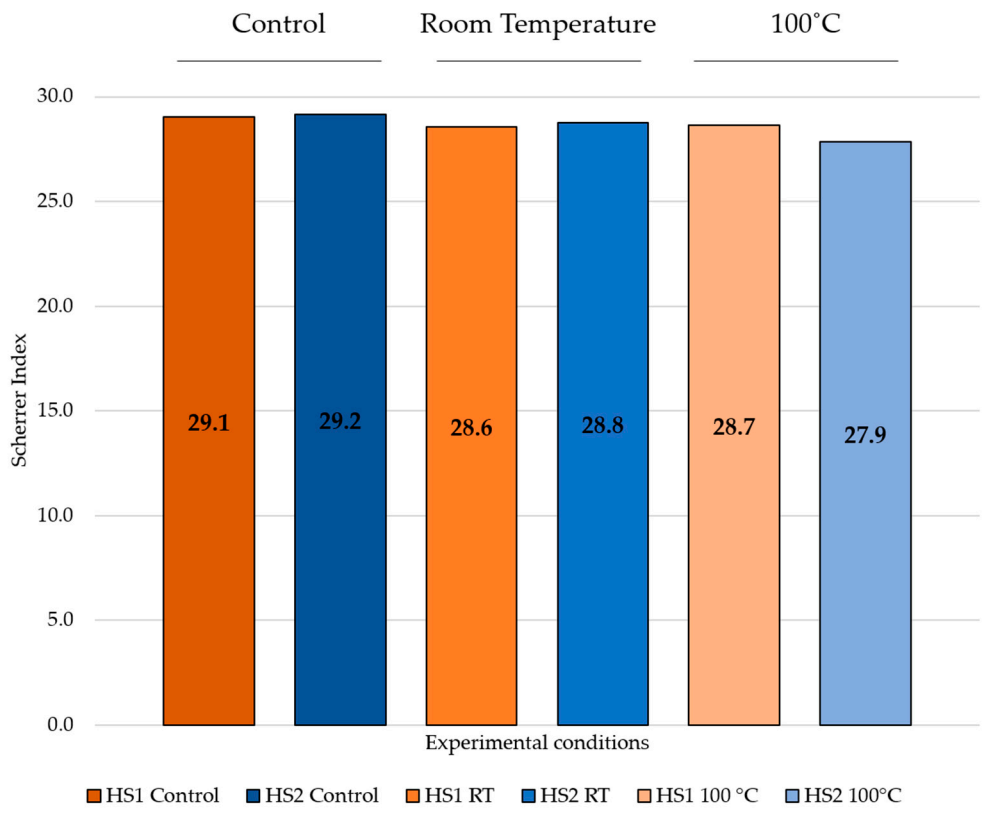

Figure 8. Percentage of crystallinity of HS1 and HS2, measured after applying the conditions of the "binderless particle board" simulation. HS1 is represented in orange shades, while HS2 is represented in shades of blue.

For HS1 (Figure 8), the crystallinity of the plant particles remains relatively stable across different extraction conditions, with the crystallinity index consistently around 29%. This stability suggests that the various extraction conditions (room temperature, RT, and 100 °C) have a minimal impact on the crystallinity of HS1.

In contrast, HS2 exhibits a slight decrease in crystallinity under different conditions. In particular, the crystallinity index for HS2 decreases from 29.2% under the control condition to 27.9% at 100 °C. This trend could indicate that the extraction conditions, particularly at higher temperatures, have a slightly greater effect on HS2 compared to HS1.

The crystallinity values for both HS1 and HS2 under control conditions are quite similar and align closely with the literature. For instance, Momeni et al. (2021) [55] reported a crystallinity percentage of 27.1% for untreated hemp shiv powder.

The impact of hot water treatment does not fully disrupt the non-crystalline components such as lignin, hemicellulose, or pectins. As a result, the plant cell wall remains largely intact, limiting access to the cellulose structure, which explains our results.

4. Conclusions

To investigate the release of plant cell wall components during the formulation of agro-based concrete and binderless particle boards, several liquid extractions were performed, varying in pH and temperature. Two types of hemp shiv, "HS1" and "HS2", were selected based on their behavior observed in previous studies [11–13]. HS1 is known to release a high quantity of extractives, which poses challenges in the formulation of agro-based concrete but may offer beneficial properties for binderless particle boards. In contrast, HS2 releases fewer extractives, making it more suitable for agro-based concrete applications, while it may be less advantageous for binderless particle boards.

In this study, both hemp shiv types were analyzed, revealing notable differences in their behavior and extractive release, as outlined below:

- Chemical Analysis:
  - Van Soest analysis indicated that HS2 contains a higher rate of lignin compared to HS1, while HS1 has a higher concentration of soluble compounds.
  - Microbial activity was slightly higher in HS2 than in HS1.
  - Mass loss and pH changes varied significantly between HS1 and HS2. At first, the increase in temperature (50 °C or 100 °C) led to a decrease in pH for HS1, while an unexpected pH rise was observed for HS2. For "agro-based concrete" simulation, NaOH was found to be a more effective extraction agent than $Ca(OH)_2$. The combined effects of pH and temperature did not significantly increase mass loss but did facilitate the release of extractive compounds. HS1 generally released more extractives than HS2, except under conditions using $Ca(OH)_2$, regardless of temperature. However, for the "binderless particle board" simulation, similitude was observed between hemp shiv, although a raise in pH units was found for HS2. The effect of temperature slightly increased the mass loss for hemp shiv, while HS1 released more compounds than HS2.
  - The pH decreased during the alkaline extraction simulation of "agro-based concrete", suggesting the release of acidic molecules potentially from sugar degradation (e.g., lactic acids) or polyphenols (e.g., hydroxycinnamic acids).
  - Some of these molecules at a lower amount could have been released during the hot water extraction simulation of the "binderless particle board", which may explain the pH decrease, especially for HS1.
- Physical and Microscopic Analysis:
  - Density measurements and SEM analysis revealed no significant differences between HS1 and HS2.
  - XRD and BET analyses showed minimal differences between HS1 and HS2, except for HS2 at 100 °C for the "binderless particle board" simulation, where there was a decrease in the specific surface area and a tendency for reduced cellulose

crystallinity. On the other hand, in the "agro-based concrete" simulation, a huge difference was observed between NaOH and $Ca(OH)_2$ without temperature contribution.

This study highlights the inherent variability of plant-based materials, which can lead to inconsistencies in their performance and properties. This variability is a significant challenge in the formulation of agro-based materials, where uniformity is often desired for predictable physical performances. This work provides insights into the liquid extraction processes and their effects on hemp shiv, but it is important to acknowledge the following limitations:

- This study primarily addresses liquid extraction parameters (pH, temperature), but overlooks key factors like pressure and humidity, which are crucial in binderless particle board performance and extractive compound release [29].
- When plant materials are used in Portland cement, crystalline phases formed during hydration can modify plant cell wall structures, potentially altering the type of extractives released [20].
- The release of extractive compounds during processing affects the properties of agro-based materials. Thus, controlling this release is vital to optimize performance.
- The variability in extractives between different plant samples, and even within the same agro-resource like hemp, suggests the need for a tailored approach and pretreatment processes to standardize materials before application [56].

Future work should focus on pretreatment methods for reducing variability, and explore factors like pressure, humidity, and time in binderless particle boards. Enhancing the Interfacial Transition Zone (ITZ) in plant particles can improve mechanical properties [65]. To fully utilize hemp shiv in construction, future studies should assess its mechanical, thermal, and environmental properties, including biodegradability and the impact on indoor air quality. This will ensure its suitability as a sustainable and versatile building material. Expanding research to include these aspects will provide a more comprehensive understanding of hemp shiv's suitability in various applications.

Author Contributions: Conceptualization, M.-S.D., H.L., V.L., P.M. and N.L.; methodology, M.-S.D., H.L., V.L., S.P., É.C. and A.H.; software, M.-S.D., H.L., S.P. and É.C.; validation, H.L., P.M. and N.L.; formal analysis, H.L. and P.M.; investigation, M.-S.D., A.H. and H.L.; resources, H.L., P.M. and N.L.; data curation, M.-S.D., H.L. and A.H.; writing—Original draft preparation, M.-S.D. and H.L.; writing—Review and editing, M.-S.D., H.L., A.H., P.M. and N.L.; supervision, H.L. and A.H.; project administration, H.L., P.M. and N.L.; funding acquisition, H.L., P.M. and N.L. All authors have read and agreed to the published version of the manuscript.

Funding: This research was funded by the Communauté d'Agglomération de Béthune Bruay Artois Lys Romane (CABBALR) in Béthune, France, and the GoLaSalle project from UniLaSalle Rouen, France, which supported Diakité's three-year PhD research.

Institutional Review Board Statement: Not applicable.

Informed Consent Statement: Not applicable.

Data Availability Statement: The data that support the findings of this study are available from the corresponding author, [M.-S.D.], upon reasonable request.

Acknowledgments: We would like to thank David Marier (UniLaSalle, France) for his contributions to the microbial activity measurements and the valuable discussions we had. We also extend our gratitude to Marianne Rosa (UTA, UniLaSalle, France) for providing the SEM images. Above all, we wish to express our deepest thanks to Hélène Lenormand. Without her, this work would never have come to fruition. From her warm smile to her kindness and expertise, we wish her eternal peace. Rest in peace, Hélène.

Conflicts of Interest: The authors declare no conflicts of interest. The funders had no role in the design of the study; in the collection, analyses, or interpretation of data; in the writing of the manuscript, or in the decision to publish the results.

References

1. La Corderie Royale de Rochefort. Available online: https://www.corderie-royale.com/ (accessed on 31 July 2024).
2. Crini, G.; Lichtfouse, E.; Chanet, G.; Morin-Crini, N. Applications of hemp in textiles, paper industry, insulation and building materials, horticulture, animal nutrition, food and beverages, nutraceuticals, cosmetics and hygiene, medicine, agrochemistry, energy production and environment: A review. *Environ. Chem. Lett.* **2020**, *18*, 1451–1476. [CrossRef]
3. Kraszkiewicz, A.; Kachel, M.; Parafiniuk, S.; Zając, G.; Niedziółka, I.; Sprawka, M. Assessment of the Possibility of Using Hemp Biomass (*Cannabis sativa* L.) for Energy Purposes: A Case Study. *Appl. Sci.* **2019**, *9*, 4437. [CrossRef]
4. Jacob, S.R.; Mishra, A.; Kumari, M.; Bhatt, K.; Gupta, V.; Singh, K. A quick viability test protocol for hemp (*Cannabis sativa* L.) seeds. *J. Nat. Fibers* **2022**, *19*, 1281–1286. [CrossRef]
5. Karche, T.; Singh, M.R. The application of hemp *Cannabis sativa* L. for a green economy: A review. *Turk. J. Bot.* **2019**, *43*, 710–723. [CrossRef]
6. Martínez Borja, V.; Mendizabal, M.B.; Roncero, E.; Bernat-Maso, E.; Gil, L. Towards sustainable building solutions: Development of hemp shiv-based green insulation material. *Constr. Build. Mater.* **2024**, *414*, 134987. [CrossRef]
7. Ahmed, A.T.M.F.; Islam, M.Z.; Mahmud, M.S.; Sarker, M.E.; Islam, M.R. Hemp as a potential raw material toward a sustainable world: A review. *Heliyon* **2022**, *8*, e08753. [CrossRef]
8. Zampori, L.; Dotelli, G.; Vernelli, V. Life cycle assessment of hemp cultivation and use of hemp-based thermal insulator materials in buildings. *Environ. Sci. Technol.* **2013**, *47*, 7413–7420. [CrossRef]
9. Pellet, R.; Marceau, S.; Diafi, D.; Tagnit-Hamou, A.; Farcas, F. Characterisation of vegetal compounds responsible for the setting delays in hydraulic binders. *Acad. J. Civ. Eng.* **2019**, *37*, 479–484.
10. Wilding, C.R.; Walter, A.; Double, D.D. A classification of inorganic and organic admixtures by conduction calorimetry. *Cem. Concr. Res.* **1984**, *14*, 185–194. [CrossRef]
11. Wang, L.; Lenormand, L.; Zmamou, H.; Leblanc, N. Effect of variability of hemp shiv on the setting of lime hemp concrete. *Ind. Crops Prod.* **2021**, *171*, 113915. [CrossRef]
12. Wang, L.; Lenormand, H.; Zmamou, H.; Leblanc, N. Effect of soluble components from plant aggregates on the setting of the lime base binder. *J. Renew. Mater.* **2019**, *7*, 903–913. [CrossRef]
13. Vinceslas, T. Caractérisation D'éco-Matériaux Terre-Chanvre en Prenant en Compte la Variabilité des Ressources Disponibles Localement. Ph.D. Thesis, University of Bretagne Sud, Vannes, France, 2019.
14. Karade, S.R. Cement-bonded composites from lignocellulosic wastes. *Constr. Build. Mater.* **2010**, *24*, 1323–1330. [CrossRef]
15. Bruere, G.M. Set-retarding effects of sugars in Portland cement pastes. *Nature* **1966**, *212*, 502–503. [CrossRef]
16. Taplin, J.H. Discussion of "some chemical additions and admixtures in cement paste and concrete". In Proceedings of the 4th International Symposium on the Chemistry of Concrete, Gaithersburg, MD, USA, 1 January 1962; Volume 2, p. 924.
17. Fischer, V.F.; Wienhaus, O.; Ryssel, M.; Oldbrecht, J. The water-soluble carbohydrates of wood and their influence on the production of lightweight wood-wools boards. *Holztechnologie* **1974**, *15*, 12–19.
18. Simatupang, M.H. Degradation reactions of glucose, cellobiose, and wood under the influence of Portland cement paste. *Holzforschung* **1986**, *40*, 149–155. [CrossRef]
19. Govin, A.; Peschard, A.; Fredon, E.; Guyonnet, R. New insights into wood and cement interaction. *Holzforschung* **2005**, *59*, 330–335. [CrossRef]
20. Diquélou, Y.; Gourlay, E.; Arnaud, L.; Kurek, B. Impact of hemp shiv on cement setting and hardening: Influence of the extracted components from the aggregates and study of the interfaces with the inorganic matrix. *Cem. Concr. Compos.* **2015**, *55*, 112–121. [CrossRef]
21. Nalet, C. Influence de la Stéréochimie et de la Fonctionnalité de Molécules Organiques sur L'hydratation de Composés Cimentaires. Ph.D. Thesis, University of Bourgogne, Dijon, France, 2015.
22. Tale Ponga, D.; Sabziparvar, A.; Cousin, P.; Boulos, L.; Robert, M.; Foruzanmehr, M.R. Retarding Effect of Hemp Hurd Lixiviates on the Hydration of Hydraulic and CSA Cements. *Materials* **2023**, *16*, 5561. [CrossRef]
23. Schäfer, M.; Roffael, E. On the formaldehyde release of wood. *Holz Roh Werkst.* **2000**, *58*, 259–264. [CrossRef]
24. Käldström, M.; Kumar, N.; Heikkilä, T.; Titta, M.; Salmi, T.; Murzin, D. Formation of furfural in catalytic transformation of levoglucosan over mesoporous materials. *ChemCatChem* **2010**, *2*, 539–546. [CrossRef]
25. Gfeller, B.; Properzi, M.; Zanetti, M.; Pizzi, A.; Pichelin, F.; Lehmann, M.; Delmotte, L. Wood bonding by mechanically induced in situ welding of polymeric structural wood constituents. *J. Appl. Polym. Sci.* **2004**, *92*, 243–251. [CrossRef]
26. Gfeller, B.; Zanetti, M.; Properzi, M.; Pizzi, A.; Pichelin, F.; Lehmann, M.; Delmotte, L. Wood bonding by vibrational welding. *J. Adhes. Sci. Technol.* **2003**, *17*, 1573–1589. [CrossRef]
27. Lamaming, J.; Sulaiman, O.; Sugimoto, T.; Hashim, R.; Said, N.; Sato, M. Influence of chemical components of oil palm on properties of binderless particleboard. *BioResources* **2013**, *8*, 3358–3371. [CrossRef]
28. Gedara, A.K.A.; Chianella, I.; Endrino, J.L.; Zhang, Q. Adhesiveless bonding of wood—A review with a focus on wood welding. *BioResources* **2021**, *16*, 6448–6470. [CrossRef]
29. Hubbe, M.; Pizzi, A.; Zhang, H.; Halis, R. Critical links governing performance of self-binding and natural binders for hot-pressed reconstituted lignocellulosic board without added formaldehyde: A review. *BioResources* **2018**, *13*, 2049–2115. [CrossRef]
30. Kang, X.; Kirui, A.; Dickwella Widanage, M.C.; Mentink-Vigier, F.; Cosgrove, D.J.; Wang, T. Lignin-polysaccharide interactions in plant secondary cell walls revealed by solid-state NMR. *Nat. Commun.* **2019**, *10*, 347. [CrossRef] [PubMed]

31. Van Soest, P.J.; Robertson, J.B.; Lewis, B.A. Methods for dietary fiber, neutral detergent fiber, and non-starch polysaccharides in relation to animal nutrition. *J. Dairy Sci.* **1991**, *74*, 3583–3597. [CrossRef] [PubMed]
32. Diakité, M.S.; Lenormand, H.; Lequart, V.; Arufe, S.; Martin, P.; Leblanc, N. Cell Wall Composition of Hemp Shiv Determined by Physical and Chemical Approaches. *Molecules* **2021**, *26*, 6334. [CrossRef] [PubMed]
33. *NF-V08-059*; Microbiologie des Aliments—Dénombrement des Levures et Moisissures par Comptage des Colonies à 25 °C—Méthode de Routine. AFNOR Edition: Saint-Denis, France, 2002. Available online: https://www.boutique.afnor.org/fr-fr/norme/nf-v08059/microbiologie-des-aliments-denombrement-des-levures-et-moisissures-par-comp/fa120539/20449 (accessed on 6 September 2024).
34. *NF EN ISO 4833-1*; Microbiology of the Food Chain—Horizontal Method for the Enumeration of Microorganisms—Part 1: Colony-Count at 30 °C by the Pour Plate Technique. AFNOR Edition: Saint-Denis, France, 2013. Available online: https://www.boutique.afnor.org/en-gb/standard/nf-en-iso-48331/microbiology-of-the-food-chain-horizontal-method-for-the-enumeration-of-mic/fa163727/42192%2020449 (accessed on 6 September 2024).
35. Amziane, S.; Collet, F.; Lawrence, M.; Magniont, C.; Picandet, V.; Sonebi, M. Recommendation of the RILEM TC 236-BBM: Characterisation testing of hemp shiv to determine the initial water content, water absorption, dry density, particle size distribution and thermal conductivity. *Mater. Struct.* **2017**, *50*, 167. [CrossRef]
36. Glé, P.; Lecompte, T.; Hélloin de Ménibus, A.; Lenormand, H.; Arufe, S.; Château, C.; Vanessa, F.; Celzard, A. Densities of hemp shiv for building: From multiscale characterization to application. *Ind. Crops Prod.* **2021**, *164*, 113390. [CrossRef]
37. Brunauer, S.; Emmet, P.H.; Teller, E. Adsorption of gases in multimolecular layers. *J. Am. Chem. Soc.* **1938**, *60*, 309–319. [CrossRef]
38. Bokhari, S.M.Q.; Chi, K.; Catchmark, J.M. Structural and physico-chemical characterization of industrial hemp hurd: Impacts of chemical pretreatments and mechanical refining. *Ind. Crops Prod.* **2021**, *171*, 113818. [CrossRef]
39. Viel, M.; Collet, F.; Lanos, C. Chemical and multi-physical characterization of agro-ressources by product as a possible raw building material. *Ind. Crops Prod.* **2018**, *120*, 214–237. [CrossRef]
40. Thomsen, A.B.; Rasmussen, S.K.; Bohn, V.; Nielsen, K.V.; Thygesen, A. *Hemp Raw Materials: The Effect of Cultivar, Growth Conditions and Pretreatment on the Chemical Composition of the Fibres*; Risø DTU-National Laboratory for Sustainable Energy: Roskilde, Denmark, 2005.
41. Garcia-Jaldon, C. Caractérisation Morphologique et Chimique du Chanvre (*Cannabis sativa*): Prétraitement à la Vapeur et Valorisation. Ph.D. Thesis, University of Joseph Fourier, Saint-Martin-d'Hères, France, 1995.
42. Vignon, M.R.; Garcia-Jaldon, C.; Dupeyre, D. Steam explosion of woody hemp chènevotte. *Int. J. Biol. Macromol.* **1995**, *17*, 395–404. [CrossRef] [PubMed]
43. Cappelletto, P.; Brizzi, M.; Mongardini, F.; Barberi, B.; Sannibale, M.; Nenci, G.; Poli, M.; Corsi, G.; Grassi, G.; Pasini, P. Italy-grown hemp: Yield, composition and cannabinoid content. *Ind. Crops Prod.* **2001**, *13*, 101–113. [CrossRef]
44. Godin, B.; Ghysel, F.; Agneessens, R.; Schmit, T.; Gofflot, S.; Lamaudière, S.; Sinnaeve, G.; Goffart, J.-P.; Gerin, P.A.; Stilmant, D.; et al. Détermination de la cellulose, des hémicelluloses, de la lignine et des cendres dans diverses cultures lignocellulosiques dédiées à la production de bioéthanol de deuxième génération. *Biotechnol. Agron. Soc. Environ.* **2010**, *14*, 549–560.
45. Gandolfi, S.; Ottolina, G.; Riva, S.; Fantoni, G.P.; Patel, I. Complete chemical analysis of carmagnola hemp hurds: Structural features of its components. *BioResources* **2013**, *8*, 2641–2656. [CrossRef]
46. Hussain, A.; Calabria-Holley, J.; Jiang, Y.; Lawrence, M. Development of novel building composites based on hemp and multi-functional silica matrix. *Compos. B* **2018**, *86*, 187–197. [CrossRef]
47. Arufe, S.; Hellouin de Menibus, A.; Leblanc, N.; Lenormand, H. Physico-chemical characterisation of plant particles with potential to produce agro-based building materials. *Ind. Crops Prod.* **2021**, *171*, 113901. [CrossRef]
48. Arufe, S.; Hellouin de Menibus, A.; Leblanc, N.; Lenormand, H. Effect of retting on hemp shiv physicochemical properties. *Ind. Crops Prod.* **2021**, *171*, 113911. [CrossRef]
49. Tarkka, M.T.; Sarniguet, A.; Frey-Klett, P. Inter-kingdom encounters: Recent advances in molecular bacterium-fungus interactions. *Curr. Genet.* **2009**, *55*, 233–243. [CrossRef] [PubMed]
50. Frey-Klett, P.; Burlinson, P.; Deveau, A.; Barret, M.; Tarkka, M.; Sarniguet, A. Bacterial-fungal interactions: Hyphens between agricultural, clinical, environmental, and food microbiologists. *Microbiol. Mol. Biol. Rev.* **2011**, *75*, 583–609. [CrossRef]
51. Fernando, D.; Thygesen, A.; Meyer, A.S.; Daniel, G. Elucidating field retting mechanisms of hemp fibres for biocomposites: Effects of microbial actions and interactions on the cellular micromorphology and ultrastructure of hemp stems and bast fibres. *BioResources* **2019**, *14*, 4047–4084. [CrossRef]
52. Nguyen, T.T.; Picandet, V.; Carre, P.; Lecompte, T.; Amziane, S.; Baley, C. Effect of Compactness on Mechanical and Thermal Properties of Hemp Concrete. *Eur. J. Environ. Civ. Eng.* **2010**, *14*, 545–560. [CrossRef]
53. Delannoy, G.; Marceau, S.; Glé, P.; Gourlay, E.; Guéguen-Minerbe, M.; Diafi, D.; Nour, I.; Amziane, S.; Farcas, F. Aging of hemp shiv used for concrete. *Mater. Des.* **2018**, *160*, 752–762. [CrossRef]
54. Mohnen, D. Pectin structure and biosynthesis. *Curr. Opin. Plant. Biol.* **2008**, *11*, 266–277. [CrossRef] [PubMed]
55. Momeni, S.; Safder, M.; Khondoker, M.A.H.; Elias, A.L. Valorization of hemp hurds as bio-sourced additives in PLA-based biocomposites. *Polymers* **2021**, *13*, 3786. [CrossRef] [PubMed]
56. Ghosn, S.; Cherkawi, N.; Hamad, B. Studies on Hemp and Recycled Aggregate Concrete. *Int. J. Concr. Struct. Mater.* **2020**, *14*, 54. [CrossRef]

57. Fantilli, A.P.; Jóźwiak-Niedźwiedzka, D.; Denis, P. Bio-Fibres as a Reinforcement of Gypsum Composites. *Materials* **2021**, *14*, 4830. [CrossRef]
58. Moine, C. Extraction, Caractérisation Structurale et Valorisation d'une Famille D'hémicellulose du Bois—Obtention de Matériaux Plastiques par Modification des Xylanes. Ph.D. Thesis, University of Limoges, Limoges, France, 2005.
59. Carpita, N.C. Fractionation of hemicelluloses from maize cell walls with increasing concentrations of alkali. *Phytochemistry* **1984**, *23*, 1089–1093. [CrossRef]
60. Bailey, R.W. Quantitative studies of ruminant digestion. *N. Z. J. Agric. Res.* **1967**, *10*, 15–32. [CrossRef]
61. Izzo, L.; Castaldo, L.; Narváez, A.; Graziani, G.; Gaspari, A.; Rodríguez-Carrasco, Y.; Ritieni, A. Analysis of phenolic compounds in commercial *Cannabis sativa* L. inflorescences using UHPLC-Q-Orbitrap HRMS. *Molecules* **2020**, *25*, 631. [CrossRef] [PubMed]
62. Tanase, C.; Volf, I.; Popa, V.I. Enhancing copper and lead bioaccumulation in rapeseed by adding hemp shives as soil natural amendments. *J. Environ. Eng. Landsc. Manag.* **2014**, *22*, 245–253. [CrossRef]
63. Tanase, C.; Băra, C.I.; Popa, V.I. Cytogenetical effect of some polyphenol compounds separated from industrial by-products on maize (*Zea mays* L.) plants. *Cellulose Chem. Technol.* **2015**, *49*, 799–805.
64. André, A.; Leupin, M.; Kneubühl, M.; Pedan, V.; Chetschik, I. Evolution of the polyphenol and terpene content, antioxidant activity and plant morphology of eight different fiber-type cultivars of *Cannabis sativa* L. cultivated at three sowing densities. *Plants* **2020**, *9*, 1740. [CrossRef]
65. Delhomme, F.; Prud'Homme, E.; Julliot, C.; Guillot, T.; Amziane, S.; Marceau, S. Effect of hemp on cement hydration: Experimental characterization of the interfacial transition zone. *Results Chem.* **2022**, *4*, 100440. [CrossRef]